PROCEEDINGS B

rspb.royalsocietypublishing.org

Research

Cite this article: Manlove K, Aiello C, Sah P, Cummins B, Hudson PJ, Cross PC. 2018 The ecology of movement and behaviour: a saturated tripartite network for describing animal contacts. *Proc. R. Soc. B* **285**: 20180670.
http://dx.doi.org/10.1098/rspb.2018.0670

Received: 27 March 2018
Accepted: 28 August 2018

Subject Category:
Behaviour

Subject Areas:
behaviour, ecology, health and disease and epidemiology

Keywords:
contact network, Lagrangian movement, tripartite tagging network, network projection, pathogen transmission

Author for correspondence:
Kezia Manlove
e-mail: kezia.manlove@gmail.com

Electronic supplementary material is available online at http://dx.doi.org/10.6084/m9.figshare.c.4219871.

THE ROYAL SOCIETY PUBLISHING

The ecology of movement and behaviour: a saturated tripartite network for describing animal contacts

Kezia Manlove[1,2], Christina Aiello[1,3], Pratha Sah[4], Bree Cummins[5], Peter J. Hudson[6] and Paul C. Cross[7]

[1]Department of Wildland Resources, Utah State University, Logan, UT, USA
[2]Department of Veterinary Microbiology and Pathology, Washington State University, Pullman, WA, USA
[3]US Geological Survey, Western Ecological Research Center, Henderson, NV, USA
[4]Center for Infectious Disease Modeling and Analysis (CIDMA), Yale School of Public Health, Yale University, New Haven, CT, USA
[5]Department of Mathematical Sciences, Montana State University, Bozeman, MT 59717, USA
[6]Center for Infectious Disease Dynamics, Pennsylvania State University, University Park, PA 16802, USA
[7]US Geological Survey, Northern Rocky Mountain Science Center, 2327 University Way, Ste. 2, Bozeman, MT 59717, USA

KM, 0000-0002-7200-5236

Ecologists regularly use animal contact networks to describe interactions underlying pathogen transmission, gene flow, and information transfer. However, empirical descriptions of contact often overlook some features of individual movement, and decisions about what kind of network to use in a particular setting are commonly *ad hoc*. Here, we relate individual movement trajectories to contact networks through a tripartite network model of individual, space, and time nodes. Most networks used in animal contact studies (e.g. individual association networks, home range overlap networks, and spatial networks) are simplifications of this tripartite model. The tripartite structure can incorporate a broad suite of alternative ecological metrics like home range sizes and patch occupancy patterns into inferences about contact network metrics such as modularity and degree distribution. We demonstrate the model's utility with two simulation studies using alternative forms of ecological data to constrain the tripartite network's structure and inform expectations about the harder-to-measure metrics related to contact.

1. Background

Animal contact networks are critical for describing the interactions that underlie pathogen transmission, gene flow, and information transfer, but empirical descriptions of contact are difficult to generate and sometimes biased [1–4]. Ecological metrics like patch occupancy and home range size require less-intensive sampling, while still retaining information about contact patterns. Incorporating these alternative information sources could improve inferences about wildlife contact network structures.

Contact patterns reflect animal behaviour. Individual space-use patterns determine which animals have opportunities to interact with one another. In gregarious species, aggregation size preferences determine how many individuals contact one another within a group. Behaviours such as territoriality or kin-based associations also contribute to the probability that individuals will interact given the opportunity.

Contacts themselves are often not directly observable. Estimated network metrics like modularity (the extent to which the network substructures into separate communities) and degree distribution (the number of connections each individual has) are often derived from incomplete information on a subset of animals. Small sample sizes and limited replication restrict the circumstances and spatio-temporal contexts to which these estimates apply [1,2].

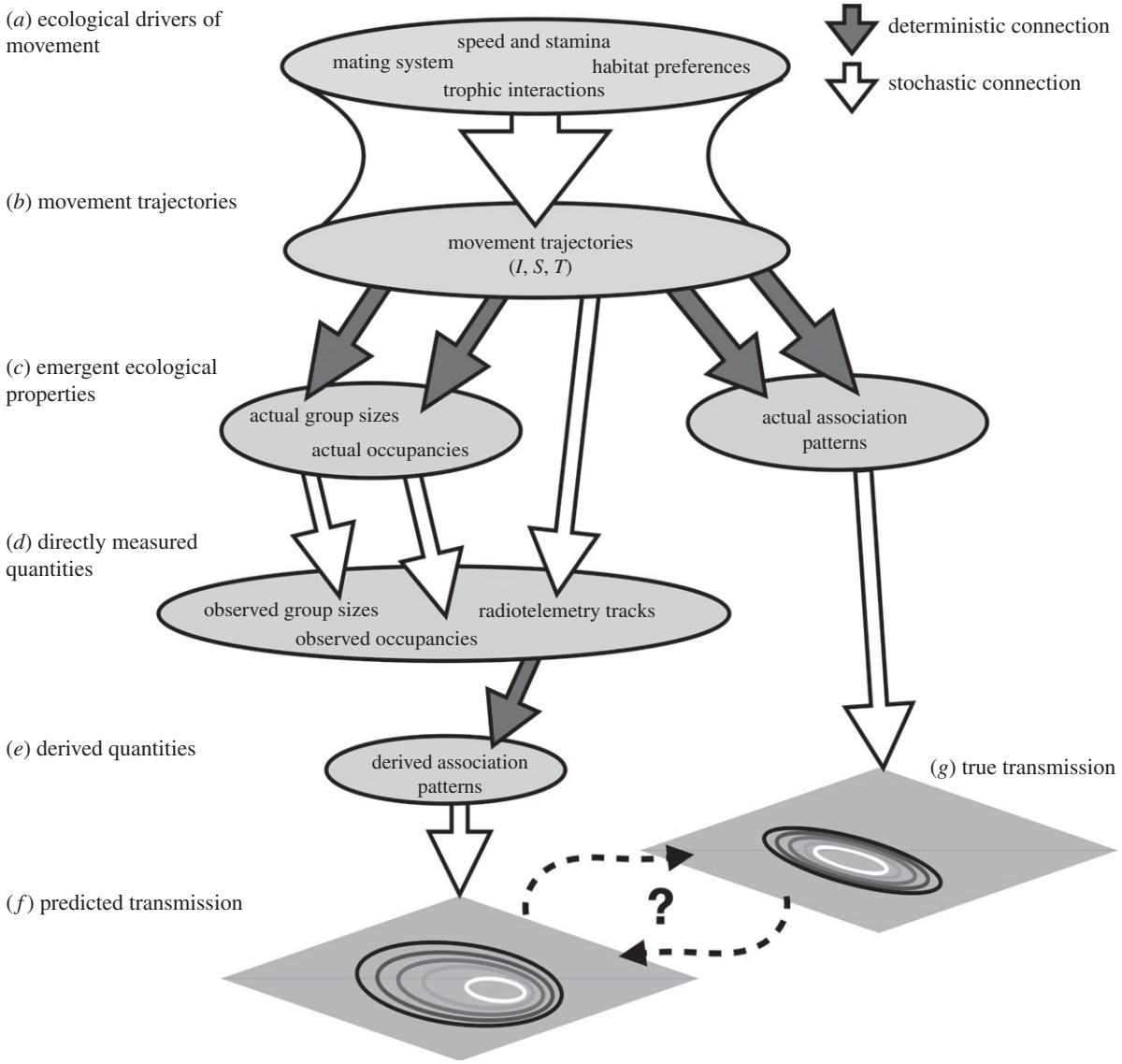

Figure 1. From movement processes to contact patterns. Overarching ecological processes in (*a*) drive a set of (realized) individual movement trajectories (*b*). These can in turn be summarized through a set of ecological features in *c*, which are fully determined by the movement trajectories describing individual identity (I), location in space (S), and position in time (T). Some ecological features can then be measured (with noise) to produce various ecological datasets (*d*). Other ecological metrics, in particular, those describing contact networks, are derived from observed ecological data (*e*). These derived network metrics are then used as a basis for simulation studies of transmission (*f*). A key question is how well these forecasted transmission dynamics match those realized in the system (*g*).

Since contact patterns are a product of spatial and behavioural preferences, behaviour and space-use data might help overcome some limitations to network inference, while also strengthening insight about ecological context. This could be particularly useful for projects whose eventual objective is to model disease transmission, gene flow, or other transfer processes that emerge from an underlying network structure. Yet despite the potential benefits of integrating other forms of information into inferences about network structure, clear strategies for directly incorporating these data are limited.

Here, we propose a mathematical framework that links contact networks with other types of ecological data. Our approach is based on a tripartite network model that explicitly describes individual identity, location, and time. First, we introduce animal movement trajectories and formalize their relationship to contacts. Then, we describe the tripartite model, and illustrate how different types of contact networks are all simplifications of the tripartite structure. Next, we demonstrate the model's utility by showing how some animal social systems generate consistent and measurable dependencies between the tripartite network's elements. Finally, we implement two simulations that illustrate how behavioural and space-use data could be integrated into simulated networks underlying studies of transmission.

2. From ecological processes to emergent patterns of contact

An animal's movement trajectory starts with its birth, ends with its death, and describes its positions in space and time between the two. Numerous internal and external processes influence the particular paths individuals take (figure 1*a*). Describing these individual movement tracks and the processes that shape them is the realm of movement ecology (figure 1*b*).

Ecological features like individual survival times, population densities, home range sizes, and connectivity patterns summarize certain aspects of movement trajectories (figure 1*c*). If movement trajectories were completely known, these features could be derived without uncertainty: they are deterministic functions of animal movements. Wildlife and behavioural ecologists often draw inferences from direct

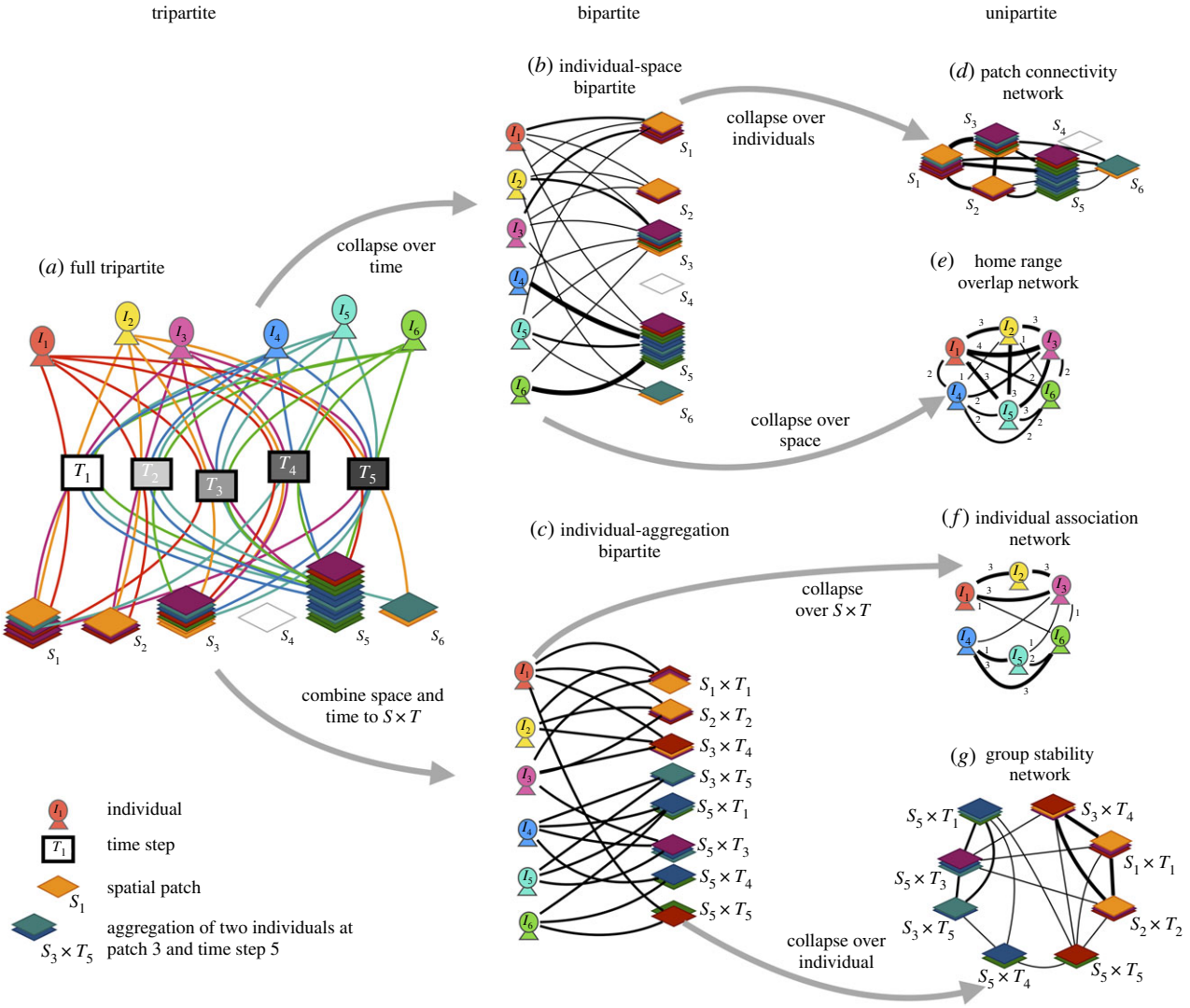

Figure 2. Network constructions project the full tripartite structure. (*a*) The full tripartite network shows how six individuals (I) occupy six spatial patches (S) over five time steps (T). Stack heights represent how often each patch was occupied, and colours indicate the occupying individuals. Curves pass through the time step of each occupation. Individuals occupy one patch at a time, but can visit the same patch multiple times. Multiple individuals can occupy the same patch simultaneously. (*b*) The individual-space bipartite network connects individuals to spatial patches they occupy. (*c*) The individual-aggregation bipartite network connects individuals to aggregations (points in space–time) in which they occur. (*d–g*) are unipartite projections of the bipartite networks in (*b*) and (*c*).

observation of these summary measurements (figure 1*d*); and ecological statisticians work to describe the uncertainty surrounding them.

Observed data regularly used to build networks, such as radiotelemetry tracks, mark-recapture schemes, proximity loggers, or video recordings, are subject to sampling variability (figure 1*d*). This variation propagates downward through all subsequent analysis: calculated network metrics (1*e*) and models for predicting transmission (1*f*) rely on a network inferred from noisy data. As a consequence, the relationship between estimated metrics and the system's true contact (1*c*) and transmission dynamics (1*g*) is uncertain. Here, our goal is to reduce that uncertainty by considering how information from other ecological data sources might be harnessed to refine empirical descriptions of contact.

3. A tripartite network of identity, location, and time

Movement trajectories can be written as three-part records describing individual identity, location in space, and position in time (directly analogous to the Lagrangian perspective in movement ecology; [5]). This three-part description naturally lends itself to a tripartite (three-part) network of Individual, Space, and Time nodes (with both Space and Time treated as discrete). A similar three-part structure, known as a folksonomy or tripartite tagging network, is used in the computer science literature to describe how users tag items and reviews online [6–9]. In our cases, edges link individuals to locations, with each edge bearing a tag that indicates when each individual-site pairing occurred (figure 2*a*).

Consider an individual, $I \in \{1, \ldots, N\}$ in a population of size N, moving across a spatial domain $D_S \subset \mathbb{R}^d$, over time $D_T \subset \mathbb{R}$. Individual locations in space and time can be written as a set of triads $\{(I, S, T)\}$, where I identifies the individual, S identifies the location in space, and T identifies the position in time. The set of all triads forms a surface completely describing the realized spatio-temporal distribution of individuals, and consequently the tripartite (I, S, T) network also provides a complete representation of the spatio-temporally explicit contact process at the specified spatial and temporal resolution.

Table 1. Common unipartite network construction methods in terms of (I, S, T). $||$ indicates magnitude (the count of the size of the set), $\{\}$ indicates a set fulfilling some condition. '$|$' is the conditioning bar and $\cap$ is the intersection symbol. $e_{ij} = ||\{(S|I = I_i) \cap (S|I = I_j)\}||$ is read as 'The number of spatial patches occupied (at any time) by individual i that were also occupied (at any time) by individual j'.

network type	(I, S, T) notation	trajectory marginal employed	nodes	edge definitions in a weighted network
home range overlap network	(I, S) aggregated over time T	$X_k = \{S\|I = I_k\}$. Set of positions in space used by individual I_k, integrated over time T	individuals (I)	$e_{ij} \propto \|\|\{(S\|I = I_i) \cap (S\|I = I_j)\}\|\|$ Edges occur in proportion to the number of patches used by individual i that are also used by individual j
patch connectivity network	(I, S) aggregated over time T	$X_k = \{I\|S = S_k\}$. Set of individual that occupied patch S_k, integrated over time T	points in space (S)	$e_{ij} \propto \|\|\{(I\|S = S_i) \cap (I\|S = S_j)\}\|\|$ Edges occur in proportion to the number of individuals visiting site i that also visit site j
individual association network	$(I, S \times T)$	$X_k = \{(S \times T)\|I = I_k\}$. Set of aggregations with I_k as a member	individuals (I)	$e_{ij} \propto \|\|\{((S \times T)\|I = I_i) \cap ((S \times T)\|I = I_j)\}\|\|$ Edges occur in proportion to the number of aggregations that include individual i that also include individual j
aggregation stability network	$(I, S \times T)$	$X_k = \{I\|(S \times T) = (S \times T)_k\}$. Set of individuals present in aggregation $(S \times T)_k$	aggregations ($S \times T$)	$e_{ij} \propto \|\|\{(I\|(S \times T) = (S \times T)_i) \cap (I\|(S \times T) = (S \times T)_j)\}\|\|$ Edges occur in proportion to the number of individuals in aggregation i that are also present in aggregation j

4. Relating the tripartite model to commonly used ecological contact networks

Edges in contact networks represent intersections in animal movement trajectories. Consider the movement trajectories of two individuals, I_1 and I_2, denoted $X_1 = \{S, T \mid I = I_1\}$ and $X_2 = \{S, T \mid I = I_2\}$. We read X_1 and X_2 as 'the set of points in space and time occupied by individual 1', and 'the set of points in space and time occupied by individual 2', respectively. The intersection of those trajectories, $X_1 \bigcap X_2$, contains all points in space and time where I_1 and I_2 co-occur—their complete set of direct contacts. The size of the intersection is proportional to the edge-weight linking that pair of individuals in an individual association network. Because X_1 and X_2 are conditioned on specific individuals, the network produced by X_1 and X_2 retains individual-specific information, and individuals form the network's nodes. Specific information about the space and time of contacts are not retained, however; contact events are simply summed up in the trajectories' intersection (figure 2*f*). Directly connecting individuals in proportion to their co-occurrence in space and time equates to 'projecting' the tripartite network down to a unipartite network only containing nodes of type I (e.g. [10]).

Restructuring the conditional term within the movement trajectories changes the network projection. For example, if $Y_1 = \{I \mid S = S_1\}$ and $Y_2 = \{I \mid S = S_2\}$, then the intersection $Y_1 \bigcap Y_2$ is the set of individuals who visited both S_1 and S_2. A network based on this conditioning retains information about specific spatial patches, which form its nodes. Edges are weighted by the number of individuals who visited both patches, but information about the specific individuals involved is lost.

Table 1 describes the projections underlying common ecological networks. The tripartite model has two reasonable bipartite projections (figure 2*b*,*c*), and four unipartite projections (figure 2*d*–*g*), most of which are at least occasionally used in ecological studies of contact.

One bipartite projection is an (I, S) projection (figure 2*b*) which aggregates over time and measures individual interactions in terms of shared space. This individual-space projection can produce two unipartite reductions. Patch connectivity networks connect sites (S) on the basis of shared individuals (I; figure 2*d*). Home range overlap networks connect individuals (I) that visit the same sites (S; figure 2*e*).

The other bipartite projection is an $(I, S \times T)$ projection (figure 2*c*), in which individuals interact with one another through presence in the same 'aggregation' (which is to say, being in the same place at the same time). Crossing space and time removes information on precisely when and where an aggregation occurred, but differentiates aggregations from one another in space–time. These networks are often generated by researchers surveying a population at fixed intervals in time, and recording group membership for each identifiable individual during each survey. The individual-aggregation bipartite structure can be reduced to two unipartite networks. An individual association network connects individuals in proportion to their occurrence in the same aggregations (figure 2*f*). A network of communities takes the opposite reduction, and connects aggregations $(S \times T)$ in proportion to their shared individuals (figure 2*g*).

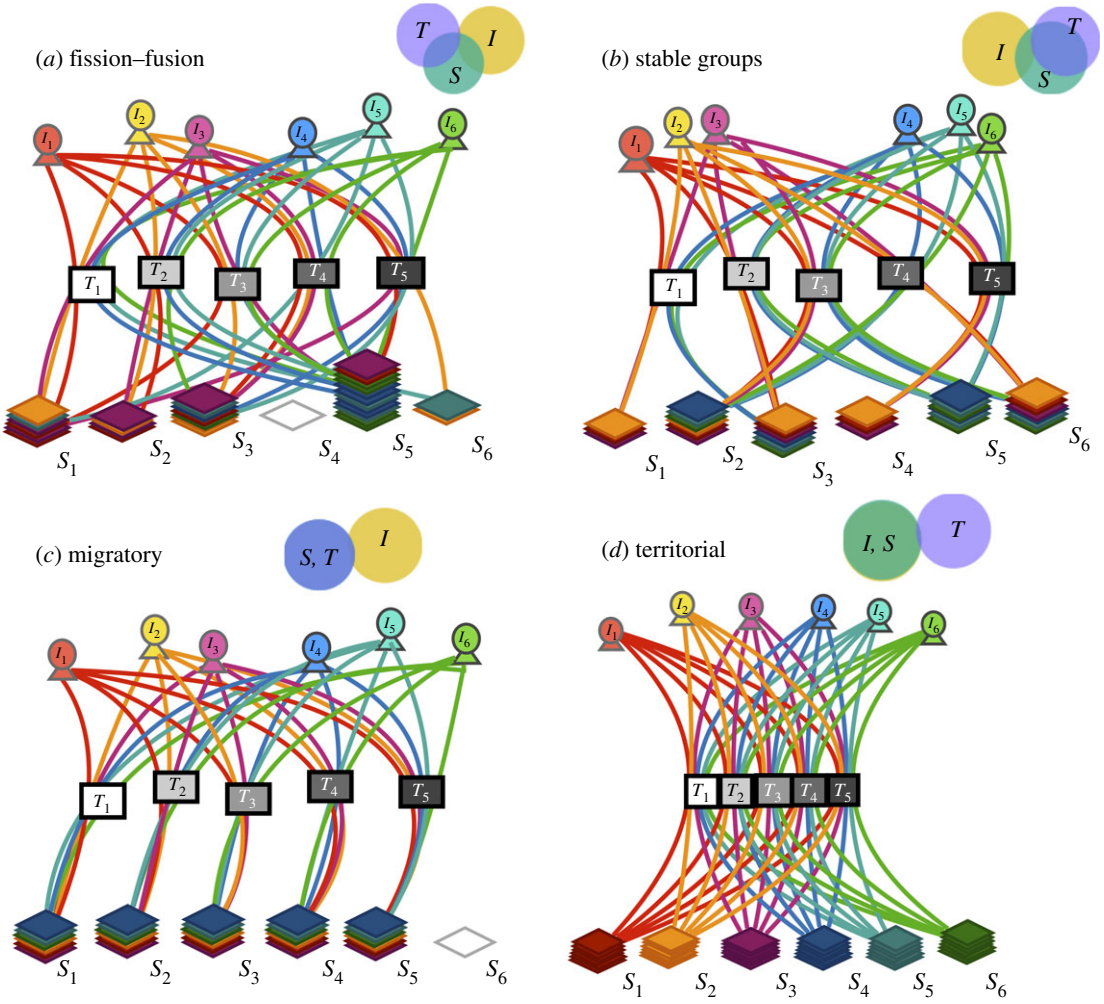

Figure 3. Animal behaviour motifs generate consistent correlations in individual identity (I), spatial location (S), and time (T). Venn diagrams show mutual information between variable pairs. Completely overlapping circles contain no independent information, whereas entirely separated circles are completely independent (see the electronic supplementary material for calculation details). (*a*) Fission–fusion societies may have low mutual information between I, S, and T. (*b*) In societies with stable social groups, locations in space and time are correlated among group members (individuals 1, 2, and 3 in one group; and 4, 5, and 6 in the other), so that an (I, $S \times T$) bipartite network captures much of the information in the full tripartite network. (*c*) In some migratory societies, locations in space are associated with positions in time, with all individuals located at the same patch in a given time. (*d*) In territorial societies, individual identity is correlated with position in space, so that unipartite projections of either individuals or locations in space capture most of the information on spatio-temporal patterns of contact. (Online version in colour.)

5. The tripartite model links animal behaviours to network projections

Condensing the full (I, S, T) tripartite network to a simpler unipartite or bipartite projection always reduces the network's information content, but the amount of information lost depends on redundancy between the I, S, and T variables [10,11]. One way to quantify information loss is through the pairwise mutual information between I, S, and T [12]. If mutual information between two variables is high, most of the information from one variable is replicated in the other. For example, sometimes knowing an individual's location provides information about its identity, and vice versa. When mutual information between variables is high, lower-dimensional networks may retain most of the information in the complete tripartite network.

Behaviour can structure the mutual information among the I, S, and T variables. For some species, good conditions may draw certain individuals together at particular points in space and time in fusion events (figure 3*a*; [13]), and drive groups to fracture when conditions decline. Species like bighorn sheep [14] or onagers [15] that exhibit this fission–fusion dynamic may have low mutual information between I, S, and T, allowing the full tripartite network to capture aspects of contact overlooked in lower-dimensional projections (figure 3*a*).

Social preferences generate correlations between individual identity and aggregation membership for species like elephants [16] that live in stable social groups which overlap in space (figure 3*b*). In these societies, two individuals either consistently co-occur in space and time if they are in the same social group, or rarely co-occur if they are in different groups. In this situation, information is shared between individuals, so that knowing one group member's location at a particular point in time provides strong insights about the contemporaneous location of its group members. High mutual information between individuals means that spatio-temporally explicit contact patterns can be captured with an (I, $S \times T$) network.

Species that undergo population-wide seasonal migrations are likely to exhibit information sharing between space and time. For these species, spatio-temporally explicit contact patterns could potentially be described in a bipartite network of (I, S) or (I, T), but including both S and T may be unnecessary.

For territorial species like damselflies [17] or wolves [18], individuals (or social groups) roughly partition space, generating high mutual information between S and I (figure 3*d*). In these societies, spatio-temporally explicit contact patterns can sometimes be captured through patch connectivity networks with spatial nodes, or individual association networks (see electronic supplementary material).

Lower-dimensional networks that exclude I, S, or T will always contain less information than the tripartite network. Researchers designing network studies are aware of, and often adjust for, perceived relationships to minimize information loss when designing network data collection, but in our experience, this integration is often *ad hoc*. Mutual information may offer researchers one route for quantitatively grounding those decisions.

In principle, the set of possible tripartite networks can be quite large, but it is often dramatically reduced if marginal distributions are known [19]. One strength of the tripartite model is that it has many well-studied and ecologically relevant margins. For instance, a distribution of patch occupancy frequencies captures the total number of time steps each patch was occupied; and a distribution of individual-level home range sizes captures the distribution of the number of unique patches each individual occupied. These and other behavioural or space-use metrics describing specific marginal distributions of the (I, S, and T) array can inform the set of possible edge configurations within the tripartite network. In practice, integrating these marginal distributions into network structures would allow researchers to draw inferences about network metrics like modularity or degree, even in the absence of movement trajectory data on a large number of individuals.

6. Simulating tripartite networks subject to marginal constraints

Marginal constraints have been used to build 'null' networks to test a variety of hypotheses about ecological networks, including biogeographic dynamics [20,21], species co-occurrence [22], and more recently, social structures (e.g. [23] and reviewed in [24]). In these studies, researchers typically simulate a random set of null networks constrained to have particular marginal distribution(s). A test statistic of interest is recorded for each simulated network. The set of test statistics generated under the null is then used as a reference distribution against which researchers compare an empirically realized test statistic value.

Here, we focus on the reference distribution itself. Multipartite network simulation hinges on drawing stubs (one-sided edges) for particular node types, and then randomly connecting stubs across node types [9,25]. For example, with a known aggregation size distribution, we might assign each individual I node one stub for each time step it was observed (an individual observed four times would get four stubs). The same total number of stubs would then be distributed across aggregation nodes, with each aggregation getting stubs equal to its observed size (an aggregation of size seven would get seven stubs). Then, we would randomly connect individual and aggregation stubs to build a bipartite individual-aggregation network, subject to individual observation frequency and aggregation size constraints. This network could then be projected down to an individual association network, and that projection could serve as a basis for calculating metrics of interest.

At the tripartite structure, simulations of the true-but-unobserved tripartite network can be constrained through summary data sources entering the simulation in two ways. First, the total number of stubs on each I, S, or T node can be drawn from an unconditional distribution of occurrence (for example, distributions of the number of times individuals were observed or the number of animal-days patches were occupied). Second, connections between nodes of different types can be specified through conditional distributions describing population features like aggregation sizes (how many individuals co-occur at a particular point in space and time, $||\{I \mid (S \times T)\}||$), individual habitat utilization patterns (how often an individual visits each patch, $||\{S = S| I = I\}||$), and patch occupancy patterns (how frequently a patch is occupied, $||\{T \mid S = S\}||$). The tripartite network is built by connecting stubs from different node types randomly, but in accordance with these conditional distributions.

Finally, we can project the tripartite network down to the desired lower-dimensional representation, and record network metrics calculated on that projection. Repeating this process many times produces a set of random contact networks subject to the specified constraints. Simulation utility is illustrated with two examples below. R code and full simulation protocols for both simulations are included with the electronic supplementary material.

(a) Example 1: generating a set of individual association network modularities from individual home range size and patch occupancy data

In the first scenario, we imagined a researcher who is interested in modelling contact, but only has data on home range sizes and patch occupancy patterns. Our goal was to generate a distribution of plausible modularities from the individual association network, subject to constraints from the researcher's data, but in the absence of radiotelemetry data documenting particular individual movement trajectories. We conducted this simulation under two different ecological contexts: first, a system in which space use was highly overdispersed, so that most patches were used very rarely, while a few were used with extremely high frequency; and second, a system in which space use was underdispersed, and all patches were used with similar frequency.

To run the simulation, we built mock datasets describing home range sizes and patch occupancy patterns in each scenario. We let the population consist of 50 individuals distributed across 30 habitat patches, and we let the process run for 40 time steps. We randomly sampled a home range size for each individual and a quality score for each patch from distributions defined by the scenario's ecological context (see electronic supplementary material for additional details). We simulated 1 000 tripartite (I, S, and T) networks subject to the home range size and patch occupancy constraints, and projected each tripartite network down to its individual association network projection. We then calculated and stored modularity values describing the proportion of within- versus between-group connections in the network generated from each simulation.

We contrasted modularity values from the individual association networks built subject to constraints with modularity values produced under a null model in which individuals

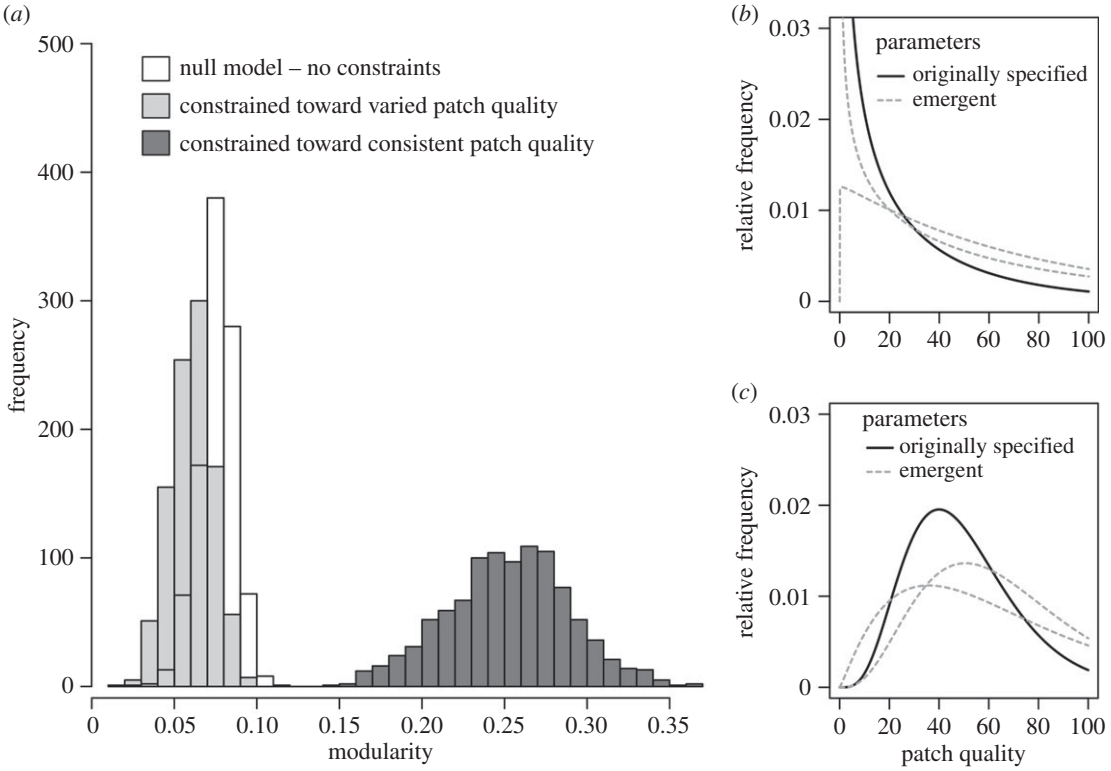

Figure 4. Home range size and patch quality data inform expectations about network topology. In the null model (white), simulated networks were not subject to any marginal constraints, but in two contrasting models (light and dark grey), networks were simulated subject to constraints from 'observed' individual home range sizes and patch occupancy patterns. In the light grey model, the system was constrained toward highly varied patch quality (distribution shown in *b*), whereas in the dark grey model, the system was constrained toward consistent patch quality (distribution shown in *c*). Each histogram contains modularity estimates from 1 000 simulated individual association networks. Panels (*b*) and (*c*) show the simulator's capacity to recapture input parameters in the overdispersed (*b*) and underdispersed (*c*) scenarios. Dashed lines in (*b*) and (*c*) show distributions based on the 2.5th and 97.5th quantiles, respectively, of maximum likelihood fits to the emergent patch quality distribution; solid lines indicate the patch quality distribution specified at the simulation's outset.

moved completely at random. Modularities under the null model and both constrained scenarios are shown in figure 4. Including marginal constraints altered the relative frequencies of the modularity values. Networks constrained by overdispersed space use tended to have lower modularities than networks generated in the absence of information, whereas the opposite was true for networks constrained to have consistent space use. In both scenarios, simulated modularities with appropriate constraints could provide the researcher an *a priori* expectation about mixing dynamics within the system, even without direct collection of network data. A complete description of the simulation protocol is provided in the electronic supplementary material.

(b) Example 2: exploring the relationship between group size, home range size, and modularity in individual associations

In the second scenario, we imagined a researcher seeking a more general description of how a set of ecological and network metrics correspond to changes in aggregation size distribution, in environments with heterogeneous habitat quality.

First, we built a series of 1 000 datasets describing aggregation size. For each dataset, we simulated a realized aggregation size distribution according to a Gamma (Shape, Scale) distribution. The shape parameter of the Gamma distribution ranged systematically from 0.5 to 50 on the log-scale, and the scale parameter ranged systematically from 2 to 10. We considered 10 increments for each parameter, giving us 100 unique distributional forms for aggregation size. We incorporated heterogeneity in patch quality by requiring patches to be occupied in a specific order (so that in time steps with five aggregations, the five top-ranked patches were occupied, but when only three aggregations were present, the 4th- and 5th-ranked patches were left empty).

We simulated 10 replicate tripartite networks under each parameter combination (see electronic supplementary material for complete protocol), and projected the tripartite networks down to their individual association network projections, where we calculated modularity. We also constructed emergent marginal distributions of the tripartite network corresponding to aggregation size and patch occupancy and recorded mean values for each. We examined simulated relationships between modularity in the individual association network, individual home range sizes, and aggregation sizes in the simulated networks.

Simulation output (figure 5) revealed systematic relationships among all three metrics. As groups became larger, modularity values of the individual association networks declined, because large groups by their very nature connect many individuals (figure 5*a*). Modularity increased with increasing home range size, presumably because larger home ranges increased the opportunity for many pairs of individuals to overlap in space (figure 5*b*). Group sizes were large when home range sizes were small in the presence of heterogeneous habitat, likely because animals all congregated at the highest-quality patches (figure 5*c*).

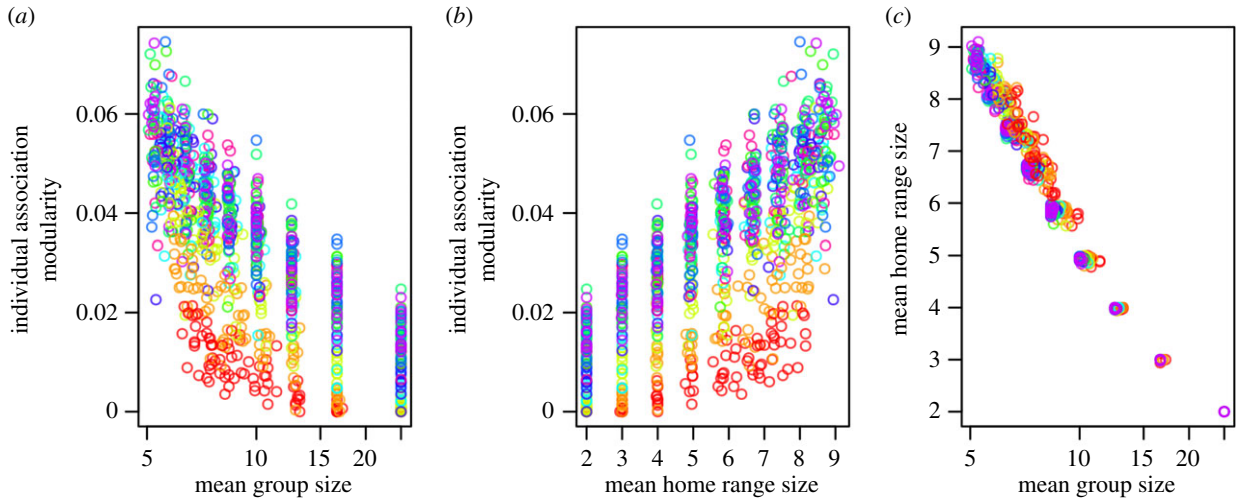

Figure 5. Aggregation size and home range size relate consistently to network modularity. (*a*) Aggregation size distribution constrained modularity of the individual association network, so that systems with larger group sizes had lower modularities. (*b*) Modularity increased with increasing home range size. (*c*) Mean group size and mean home range size were strongly related, with larger group sizes occurring in systems with small home ranges. Colours represent values of the shape parameter in the aggregation size distribution used for network simulation (red = 0.5 to blue = 50; the distribution is exponential when the shape parameter is 1, skewness declines as the value of the shape parameter increases).

7. Discussion, limitations, and conclusion

Accurately describing animal contact patterns is essential for modelling transmission of diseases, genes, and signals. Here, we propose a tripartite network model that relates network construction methods to one another and integrates contact data with other commonly collected ecological metrics. Our approach offers a way to incorporate a variety of summary data sources into contact network construction to validate and strengthen inferences about patterns of contact and transmission.

Many authors have considered more than one variable of the tripartite model in contact analyses (e.g. [26–33]), and some have made headway toward considering all three (e.g. [34–36]). Our approach rests on the foundation of this work, but at least four major limitations remain: the tripartite model requires discretization of space and time; it assumes that contacts described in the network accurately approximate contacts required for transmission; and it overlooks observation errors associated with the data. Lastly, simulation under the tripartite model remains a challenge. We briefly address each of these below.

(a) Limitation 1: discretizing space and time produces information loss

The tripartite model requires discretizing space and time. Discretization at any scale results in information loss from the continuous movement process, with the amount of information lost depending on the scale of autocorrelation across space and time. Autocorrelation is driven in turn by the spatio-temporal movement dynamics of the system [37]. When measurements are rapid relative to movement rates (i.e. animals rarely move between discrete spatial patches in consecutive observations), coarsening the scale may result in minimal information loss. However, if animals regularly move across multiple patches between consecutive observations, information loss could be high. Matching discretization to the spatial and temporal scales of movement is probably the most efficient way to capture contact patterns. Networks built on discretization at appropriate resolutions should retain most of the information of the continuous movement process, but this issue merits further exploration.

(b) Limitation 2: transmission dynamics also depend on order of occupancy, and on characteristics of the transmitted entity

Host contact patterns are crucial for understanding transmission dynamics, but they may not provide accurate predictions of transmission unless they also account for certain features of the pathogen, gene, or signal being transmitted. Often, hosts only release transmissible entities like seeds, pathogens, or signals into the environment during certain times, for example, during infectious periods, signalling periods, or periods of oestrus. The duration of the transmission period couples with the host's movement rate to determine when and where an animal transmits. Some transmission events are well-approximated by host movements, but in other situations, signals, seeds, and pathogens can persist and move long distances outside the host. These independent movements extend the region of transmission beyond the host's movement trajectory (e.g. [35,38]). How these independent movements alter the contact structure relevant for transmission is a topic of on-going investigation [39–42].

When the transmissible element can persist and move outside the host, the temporal order of animal space use becomes important. If two animals visit a patch in sequence, transmission can only occur from the first to the second visitor, not from the second to the first. Incorporating persistence and movement of transmissible elements outside the host requires us to acknowledge autocorrelations within the sets of space and time nodes. Here, we treated nodes in space and nodes in time as completely independent of one another, and relaxing this assumption to allow for spatial and temporal autocorrelation is a key next step. Other authors have begun to deal with autocorrelation in spatial networks [35], and additional efforts in this area would improve models of spatio-temporal transmission patterns.

(c) Limitation 3: estimated metrics are subject to observation error

Here, we focused on deterministic relationships between different metrics generated from individual movement trajectories, without considering error in the data collection processes: our simulations explore constraints that summary data sources could place on network metrics in the presence of perfect information. These constraints are fully determined if the individual movement trajectory is known. In the presence of noise, however, their capacity to reduce uncertainty in underlying parameters would be reduced. Understanding that reduction will be important, for both measuring mutual information from field data, and applying marginal constraints to network simulations. One advantage of incorporating ecological summary datasets, however, is that they bring more information into the model, which should eventually limit the consequences of observation error.

(d) Limitation 4: not all networks are easily simulated

The simulation protocols explored here are intended to serve as toy examples that demonstrate the utility of the tripartite network structure for incorporating ecological constraints. They are by no means exhaustive, and we caution that additional work is needed to develop rigorous simulation protocols that behave appropriately across a wide variety of marginal distributions.

8. Conclusion

An integrated approach to contact and movement is crucial for advancing behavioural, movement, and disease ecology. The tripartite network model proposed here offers a preliminary integration of these fields. In its current form, the model has two clear utilities. First, the model makes explicit the role that associations between node types can play in shaping information lost through network projection. We suggest that measuring mutual information between the different node types (I, S, and T) could provide a quantitative basis for choosing which network projection should underlie simulation studies of transmission. Second, we showed how the model can incorporate ecological summary datasets to generate *a priori* expectations about contact dynamics in the absence of conventional data. Both of these utilities could be directly applied to network analyses of empirical data.

Additionally, we see this model as a scaffold for characterizing how animal behaviours map to correlation structures between individual identity, space, and time; and how these in turn relate to the information contained in different network projections. At the very least, the model provides a conceptual organization for researchers working at the movement–contact interface. We hope this exploration motivates more discussion of how to formalize that interface for the benefit of movement, behavioural, and disease ecology going forward.

Data accessibility. Code is included in the electronic supplementary material, as an appendix to the electronic supplementary material text and in two independent R scripts, TriSim_Runfile_PRSB.txt and TriSim_RequiredFuns_PRSB.txt. All data presented in the manuscript are derived from simulations included in the scripts.

Authors' contributions. All authors contributed to model development. K.M. drafted the manuscript and all authors made substantial contributions to revisions across multiple drafts.

Competing interests. We have no competing interests.

Funding. K.M. was supported on a Penn State Academic computing fellowship. C.A. and P.S. were supported through National Science Foundation Ecology of Infectious Diseases grant #1216054.

Disclaimer. Any mention of trade, firm, or product names is for descriptive purposes only and does not imply endorsement by the US Government.

References

1. Haddadi H, King AJ, Wills AP, Fay D, Lowe J, Morton AJ, Hailes S, Wilson AM. 2011 Determining association networks in social animals: choosing spatial–temporal criteria and sampling rates. *Behav. Ecol. Sociobiol.* **65**, 1659–1668. (doi:10.1007/s00265-011-1193-3)
2. Cross PC, Creech TG, Ebinger MR, Heisey DM, Irvine KM, Creel S. 2012 Wildlife contact analysis: emerging methods, questions, and challenges. *Behav. Ecol. Sociobiol.* **66**, 1437–1447. (doi:10.1007/s00265-012-1376-6)
3. Fournet J, Barrat A. 2017 Estimating the epidemic risk using non-uniformly sampled contact data. *Sci. Rep.* **7**, 9975.
4. Rocha LE, Masuda N, Holme P. 2017 Sampling of temporal networks: Methods and biases. *Phys. Rev. E* **96**, 052302. (doi:10.1103/PhysRevE.96.052302)
5. Nathan R, Getz WM, Revilla E, Holyoak M, Kadmon R, Saltz D, Smouse PE. 2008 A movement ecology paradigm for unifying organismal movement research. *Proc. Natl Acad. Sci. USA* **105**, 19 052–19 059. (doi:10.1073/pnas.0800375105)
6. Mika P. 2005 Ontologies are us: a unified model of social networks and semantics. *International Semantic Web Conference* **3729**, 522–536.
7. Lambiotte R, Ausloos M. 2006 Collaborative tagging as a tripartite network. *Comput. Sci. ICCS* **2006**, 1114–1117.
8. Lu C, Chen X, Park EK. 2009 *Exploit the tripartite network of social tagging for web clustering*. In *Proc. of the 18th ACM Conf. on Information and knowledge management 2009*, pp. 1545–1548. New York, NY: ACM.
9. Chojnacki S, Kłopotek MA. 2012 Scale invariant bipartite graph generative model. In *Security and Intelligent Information Systems*, pp. 240–250. Berlin, Heidelberg, Germany: Springer.
10. Ramasco JJ, Morris SA. 2006 Social inertia in collaboration networks. *Phys. Rev. E* **73**, 016122. (doi:10.1103/PhysRevE.73.016122)
11. Zhou T, Ren J, Medo M, Zhang YC. 2007 Bipartite network projection and personal recommendation. *Phys. Rev. E* **76**, 046115. (doi:10.1103/PhysRevE.76.046115)
12. Cover TM, Thomas JA. 1991. *Elements of information theory*. New York, NY: Wiley.
13. Sutherland WJ. 1983 Aggregation and the ideal free distribution. *J. Anim. Ecol.* **52**, 821–828. (doi:10.2307/4456)
14. Vander Wal E, Yip H, McLoughlin PD 2012 Sex-based differences in density-dependent sociality: an experiment with a gregarious ungulate. *Ecology* **93**, 206–212. (doi:10.1890/11-0020.1)
15. Sundaresan SR, Fischhoff IR, Dushoff J, Rubenstein DI. 2007 Network metrics reveal differences in social organization between two fission–fusion species, Grevy's zebra and onager. *Oecologia* **151**, 140–149. (doi:10.1007/s00442-006-0553-6)
16. Wittemyer G, Douglas-Hamilton I, Getz WM. 2005 The socioecology of elephants: analysis of the processes creating multitiered social structures. *Anim. Behav.* **69**, 1357–1371. (doi:10.1016/j.anbehav.2004.08.018)
17. Plaistow S, Siva-Jothy MT. 1996 Energetic constraints and male mate-securing tactics in the damselfly *Calopteryx splendens xanthostoma*

(Charpentier). *Proc. R. Soc. Lond. B* **263**, 1233–1239. (doi:10.1098/rspb.1996.0181)
18. Almberg ES, Cross PC, Dobson AP, Smith DW, Hudson PJ. 2012 Parasite invasion following host reintroduction: a case study of Yellowstone's wolves. *Phil. Trans R. Soc. B* **367**, 2840 (doi:10.1098/rstb.2011.0369)
19. Snijders TA. 1991 Enumeration and simulation methods for 0–1 matrices with given marginals. *Psychometrika* **56**, 397–417. (doi:10.1007/BF02294482)
20. Diamond JM, Gilpin ME. 1982 Examination of the "null" model of Connor and Simberloff for species co-occurrences on islands. *Oecologia* **52**(1), 64–74.
21. Gilpin ME, Diamond JM. 1982 Factors contributing to non-randomness in species co-occurrences on islands. *Oecologia* **52**, 75–84. (doi:10.1007/BF00349014)
22. Gotelli NJ. 2000 Null model analysis of species co-occurrence patterns. *Ecology* **81**, 2606–2621. (doi:10.1890/0012-9658(2000)081[2606:NMAOSC]2.0.CO;2)
23. Whitehead H. 2009 SOCPROG programs: analysing animal social structures. *Behav. Ecol. Sociobiol.* **63**, 65–78. (doi:10.1007/s00265-008-0697-y)
24. Farine DR. 2017 A guide to null models for animal social network analysis. *Methods Ecol. Evol.* **8**, 1309–1320. (doi:10.1111/2041-210X.12772)
25. Bejder L, Fletcher D, Bräger S. 1998 A method for testing association patterns of social animals. *Anim. Behav.* **56**, 719–725. (doi:10.1006/anbe.1998.0802)
26. Craft ME, Volz E, Packer C, Meyers LA. 2011 Disease transmission in territorial populations: the small-world network of Serengeti lions. *J. R. Soc. Interface* **8**, 776–786. (doi:10.1098/rsif.2010.0511)
27. Pinter-Wollman N *et al.* 2013 The dynamics of animal social networks: analytical, conceptual, and theoretical advances. *Behav. Ecol.* **25**, 242–255. (doi:10.1093/beheco/art047)
28. Best EC, Dwyer RG, Seddon JM, Goldizen AW. 2014 Associations are more strongly correlated with space use than kinship in female eastern grey kangaroos. *Anim. Behav.* **89**, 1–10. (doi:10.1016/j.anbehav.2013.12.011)
29. Castles M, Heinsohn R, Marshall HH, Lee AE, Cowlishaw G, Carter AJ. 2014 Social networks created with different techniques are not comparable. *Anim. Behav.* **96**, 59–67. (doi:10.1016/j.anbehav.2014.07.023)
30. Aplin LM *et al*. 2015 Consistent individual differences in the social phenotypes of wild great tits, *Parus major*. *Anim. Behav.* **108**, 117–127. (doi:10.1016/j.anbehav.2015.07.016)
31. Nunn CL, Jordán F, McCabe CM, Verdolin JL, Fewell JH. 2015 Infectious disease and group size: more than just a numbers game. *Phil. Trans. R. Soc B* **370**, 20140111. (doi:10.1098/rstb.2014.0111)
32. Pinter-Wollman N, Fiore SM, Theraulaz G. 2017 The impact of architecture on collective behaviour. *Nat. Ecol. Evol.* **1**, s41. (doi:10.1038/s41559-017-0111)
33. Spiegel O, Leu ST, Bull CM, Sih A. 2017 What's your move? Movement as a link between personality and spatial dynamics in animal populations. *Ecol. Lett.* **20**, 3–18. (doi:10.1111/ele.12708)
34. Spiegel O, Leu ST, Sih A, Bull CM. 2016 Socially interacting or indifferent neighbours? Randomization of movement paths to tease apart social preference and spatial constraints. *Methods Ecol. Evol.* **7**, 971–979. (doi:10.1111/2041-210X.12553)
35. Richardson TO, Gorochowski TE. 2015 Beyond contact-based transmission networks: the role of spatial coincidence. *J. R. Soc. Interface* **12**, 20150705. (doi:10.1098/rsif.2015.0705)
36. Richardson TO, Giuggioli L, Franks NR, Sendova-Franks AB. 2017 Measuring site fidelity and spatial segregation within animal societies. *Methods Ecol. Evol.* **8**, 965–975. (doi:10.1111/2041-210X.12751)
37. Cressie N, Wikle CK. 2015 *Statistics for spatio temporal data*. New York, NY: John Wiley & Sons.
38. Grear DA, Luong LT, Hudson PJ. 2013 Network transmission inference: host behavior and parasite life cycle make social networks meaningful in disease ecology. *Ecol. Appl.* **23**, 1906–1914. (doi:10.1890/13-0907.1)
39. Volz E, Meyers LA. 2007 Susceptible–infected–recovered epidemics in dynamic contact networks. *Proc. R. Soc. B* **274**, 2925–2934. (doi:10.1098/rspb.2007.1159)
40. Leu ST, Kappeler PM, Bull CM. 2010 Refuge sharing network predicts ectoparasite load in a lizard. *Behav. Ecol. Sociobiol.* **64**, 1495–1503. (doi:10.1007/s00265-010-0964-6)
41. VanderWaal KL, Atwill ER, Hooper S, Buckle K, McCowan B. 2013 Network structure and prevalence of *Cryptosporidium* in Belding's ground squirrels. *Behav. Ecol. Sociobiol.* **67**, 1951–1959. (doi:10.1007/s00265-013-1602-x)
42. Sih A, Spiegel O, Godfrey S, Leu S, Bull CM. 2017 Integrating social networks, animal personalities, movement ecology and parasites: a framework with examples from a lizard. *Anim. Behav.* **136**, 195–205. (doi:10.1016/j.anbehav.2017.09.008)